Clays and Clay Minerals, Vol. 50, No. 3, 371–380, 2002.

CRYSTAL-SIZE DISTRIBUTIONS OF CLAYS DURING EPISODIC DIAGENESIS: THE SALTON SEA GEOTHERMAL SYSTEM

JIN-WOOK KIM[1] AND DONALD R. PEACOR[2]

[1] Naval Research Laboratory, Code 7431, Stennis Space Center, Mississippi 39529, USA
[2] Department of Geological Sciences, The University of Michigan, Ann Arbor, Michigan 48109, USA

Abstract—Crystal-size distributions (CSDs) for clay minerals with depth were measured from the Salton Sea Geothermal Field (SSGF) as a test for the presence and meaning of theoretical crystal-size distributions in a natural system. The SSGF is a classic open hydrothermal system, and crystals are forming directly without apparent modification of early-formed crystals, over a wide range of temperature. Thus, the measured CSDs are the actual distributions for a single episode in which all crystals grew at the same time from solution at different temperatures and depths, rather than through modifications of shallower samples.

Some TEM images of ion-milled samples from a range of depths were used to measure the crystal thicknesses of illite, chlorite and biotite. Grain-size histograms flatten, broaden and shift to larger sizes with increasing depth. Values of α and β were calculated and used to verify that the measured distributions are log normal. Reduced grain-size distributions for illite in SSGF samples obey steady-state constraints.

The observations appear to be consistent with evolution of illite with increasing depth in the SSGF system by growth in an open system giving rise to log-normal distributions, followed by supply-controlled growth in an open system. Because crystals at different depths grew simultaneously under different temperature and fluid conditions as a function of depth, they do not represent different stages of a single evolving system. The relations imply that isochemical and isothermal systems which permit an evolving system to be sampled are rare or non-existent. The data for distributions for a given depth in the SSGF are consistent with growth in an open system. The collective relations therefore imply that caution should be used in interpreting conditions of crystal growth in natural systems even where CSDs give results which are necessary for, but not sufficient to prove, a given modeled mechanism.

Key Words—Closed System, Episodic Diagenesis, Illite, Log-normal Distribution, Open System, Ostwald Ripening, TEM

INTRODUCTION

For a decade or more there has been a surge in interest among clay mineralogists in relating crystal-size distributions to growth mechanisms in general, and specifically in applying the theory of Ostwald ripening as a growth mechanism of clay minerals in pelitic rocks undergoing diagenesis (*e.g.* Eberl *et al.*, 1990, 1998; Lanson and Champion, 1991; Inoue *et al.*, 1988; Jahren, 1991). That was in part prompted by the results of Baronnet (1982) who demonstrated through laboratory experiments that the size of phlogopite crystals could increase by that mechanism. Inoue *et al.* (1988) noted that Ostwald ripening could be an important process in the formation of illite from reactant smectite in hydrothermal systems. They measured grain widths and lengths as a function of expandability of smectite layers, the normalized results being consistent with steady-state profiles as predicted by Ostwald ripening theory as interpreted at that time. Eberl and Środoń (1988) obtained mean particle thicknesses and particle-thickness distributions for sericite from the Silverton Caldera, whereas Eberl *et al.* (1990) analyzed size distributions of clays and other minerals based on interpretations of X-ray diffraction (XRD), transmission electron microscope (TEM), and scanning electron microscope (SEM) data. They concluded that Ostwald ripening was a significant process in the maturation of clay minerals. Jahren (1991) showed that crystal-size distributions (CSDs) for chlorite from North Sea sediments, as obtained using scanning electron microscopy, give a steady-state profile as predicted by Ostwald ripening theory. Lanson and Champion (1991) measured crystal populations by analysis of TEM and SEM images, showing that grain-size distributions skewed to larger grain sizes with depth, as predicted by the Ostwald ripening process.

Eberl *et al.* (1998) subsequently noted that CSDs, as determined by one-dimensional or linear measures of size, tend to have a log-normal form which can only be generated by the law of proportionate effect. They postulated five growth mechanisms and derived the theoretical distributions for each. This implied substantial modification of the notions regarding so-called Ostwald ripening as described by Eberl *et al.* (1990). As defined by Ostwald (1900), Ostwald ripening is a process by which the size distribution of an existing assemblage of crystals is modified by simultaneous dissolution of fine crystals of a given phase and increase in the size of others of the same phase, at constant temperature in a system which is closed in the strict

* E-mail address of corresponding author:
jkim@nrlssc.navy.mil

thermodynamic sense (see below). A key aspect of Ostwald ripening is that it is not a process of crystal growth, strictly speaking; rather, it concerns modification of an existing, primary, distribution of crystal sizes. Moreover, it requires isothermal and closed systems, two conditions which are generally incompatible with diagenesis and low-grade metamorphism. Eberl *et al.* (1998) generalized the notion of ripening, in that three of their growth mechanisms concerned modification of pre-existing CSDs. These included supply-controlled growth, Ostwald ripening and random ripening. Ostwald ripening was described as being unrelated to log normal distributions, in which supply-controlled Ostwald ripening modifies previously-formed log normal distributions becoming more symmetrical as ripening occurs. Although not defined as such by Eberl *et al.* (1998), the relations imply that temperature must be constant, although that relation is a defined constraint for Ostwald ripening. In addition, Eberl *et al.* (1998) defined systems as open or closed in ways different from those defined conventionally, and as required of Ostwald ripening (see below for discussion).

The relations regarding determination of growth mechanisms are, however, subject to many problems. First, there is the problem of defining the growth boundaries of entities (*i.e.* 'crystals') as a result of growth processes, *i.e.* the relation between the sizes of particles in separates obtained, *e.g.* for analysis by XRD, and those of original rocks is subject to debate (*e.g.* Peacor, 1998; Li *et al.*, 1998). Second, where particle sizes are measured using XRD patterns, there is considerable disagreement about the accuracy of such measurements (*e.g.* Árkai *et al.*, 1996). Third, there is a question as to whether such theoretically-derived relations are both necessary and sufficient for conclusions regarding crystal-growth mechanisms and determination of system openness or closure in natural geological systems, *i.e.* even where observations of CSDs in natural systems are in agreement with theory, the same consistency may occur for other theoretical relations. Such was the case, for example, with relations for Ostwald ripening (Eberl *et al.*, 1990) which were subsequently modified by those of Eberl *et al.* (1998). Lastly, it is necessary to test rigorously such theories in systems which are as simple and well-known as possible with respect to actual growth mechanisms and geological conditions, especially temperature, duration, lack of overprint by subsequent events, and degree of openness to fluids and other components.

We therefore chose to study size distributions in a sequence of shales and siltstones from the Salton Sea Geothermal Field (SSGF), California, ranging from the earliest stages of diagenesis through greenschist-facies metamorphism at greatest depth (Muffler and White, 1969). This system is a classic open system in which the elevated geothermal gradient has given rise to a system of convected fluids that have caused "hydrothermal metamorphism" of the sediments (Helgeson, 1968; Muffler and White, 1969). The age of the SSGF, determined by K-Ar methods, is ~16,000 y (Kistler and Obradovich, in Muffler and White, 1969), demonstrating that the system is young and active, and the crystals have attained their present state through direct growth, unmodified by later events. The SSGF is an ideal open system. Active geothermal fluids constantly introduce additional quantities of components. G. Giorgetti (pers. comm.) studied the evolution of mineral assemblages and textures and concluded that textural and mineralogical changes are due to the direct dissolution of detrital phases and neocrystallization of authigenic phyllosilicates in pore space; *i.e.* no 'ripening' of clay minerals occurred. The geological processes in the hydrothermal-metamorphic sequence involved direct crystallization from solution, with crystal-size distributions a function of variable temperature and composition of convecting fluids as a function of depth. Thus, the measured crystal-size distributions are the actual distributions for hydrothermal metamorphism in which neocrystallization occurs at the same time at all depths from solution, rather than through time-dependent transformations with increasing depth. This system is therefore geologically simple and well defined.

Two prograde sequences of samples have been studied in our laboratory (Yau *et al.*, 1987, 1988; Donaghe and Peacor, 1987) using TEM. Hundreds of TEM images from those studies that recorded crystal sizes were available. We utilized the images to determine CSDs and relate those data to theories of crystal growth.

SAMPLES AND EXPERIMENTAL METHODS

The TEM images used in this study were obtained from samples of shale cuttings from two wells in the Salton Sea area, California. One is the main well of the Salton Sea Scientific Drilling Project (SSSDP), C S 2-14 well, with samples from depths of 390.9, 446.4, 548.7, 744 and 1572.6 m and the other is the No. 2 Imperial Irrigation District (IID No. 2) well, with samples from depths of 485.5 and 1242.9 m. Depths and corresponding temperatures for the IID No. 2 well are: 250–1360 meters below surface (mbs) (115–220°C), 1360–1510 mbs (220–310°C), >1560 mbs (>310°C) for the zones dominated by illite, chlorite and biotite, respectively (Giorgetti *et al.*, 2001). Images were obtained by Yau and Donaghe using the methods described by Yau *et al.* (1987, 1988).

Hundreds of illite and chlorite grain sizes were measured on the photographic negatives of lattice-fringe images from each depth using a microfiche reader, with linear scale standardized using lattice-fringe images of well-characterized compounds. Lattice fringes of illite (1.0 nm spacing) and chlorite (1.4 nm) are readily distinguished on the microfiche reader without ambi-

guity as shown in Figure 1. Most measurements were accomplished by counting 1.0 nm or 1.4 nm fringes parallel to **c*** across well-defined grain boundaries. Yau *et al.* (1987) showed that illite in Salton Sea shales occurs mainly as individual, euhedral-to-subhedral, pseudohexagonal crystals in open pore-space. Therefore, there are few uncertainties in defining the boundaries of individual crystals. Packets rarely occurred as stacks, as is common for clay minerals in shales and bentonites. In such stacks, boundaries were defined by small-angle boundaries defined, in turn, by concentrations of edge dislocations, tapering fringes in sequences of layers, boundaries between two different minerals, or strong image contrast between lattice fringes as shown in Figure 2 (see arrows). Because 001 lattice fringes of smectite, which have collapsed in the ion mill or TEM environment, have spacings equal to those of illite, ambiguity may exist in identification of illite, such that the thicknesses of crystallites with smectite interlayers would be measured as smaller than their true values in original rocks. As shown by Yau *et al.* (1987) and Giorgetti *et al.* (2001) for samples at depths equal to or greater than those of this study, however, smectite-like interlayers are uncommon or undetectable. Where they occur, they are readily identified as I-S with characteristic textural features, including occurrence as replacements of large detrital mica grains. Authigenic illite, on the other hand, was observed to occur as subhedral to euhedral crystals of characteristic shape and size with no detectable smectite interlayers. Measurements of the thicknesses of crystals of illite are therefore free of the influence of contraction of smectite in the environment of the ion mill or TEM.

The histograms of grain-size distributions were made by counting for a given grain-size range. Normalized grain-size distributions were then determined for new reduced coordinates with frequency divided by maximum frequency and thickness divided by mean-thickness, based on LSW (Lifshitz, Slyozov and Wagner) theory. The S-PLUS package of statistical programs was used to calculate log-normal distribution profiles for each depth, and observed grain-size distributions were plotted on the calculated functions. Data for χ^2 tests (Davis, 1973; Krumbein and Graybill, 1965) of distributions of observed and calculated values are summarized in Table 1.

The TEM observations were made using a JEOL 100CX TEM fitted with a scanning system and a solid-state detector and computer system in the Electron Microbeam Analysis Laboratory at the University of Michigan.

RESULTS

Histograms in Figure 3a–e display the grain-size distributions of illite at depths of 390.6, 446.4, 548.7 and 744 m and biotite at 1572.6 m, respectively, for samples from the main drill core of the SSSDP well C S 2-14. Grain-size histograms for illite at all four depths are plotted together in Figure 3f, for direct comparison. The grain-size distributions flatten, broaden and shift to greater sizes with increasing depth as predicted for Ostwald ripening (Nielsen, 1964). The mean crystal thickness of illite increases, but only by 0.7 nm from 390.6 to 744 m. The size distribution for biotite shows a well-defined population ranging in thickness from 3.0 to 200 nm.

Another set of grain-size histograms for illite from depths of 485.5 and 1242.9 m, and chlorite, from 485.5 m, from the No. 2 Imperial Irrigation District (IID No. 2) well, are plotted in Figure 4a–c. Figure 4d compares the histograms of illite for both depths, the differences again being those predicted for Ostwald ripening. The difference in mean illite crystal thickness is only 1.9 nm. The histogram for chlorite (Figure 4c) is bimodal, probably as a result of coalescence of smaller

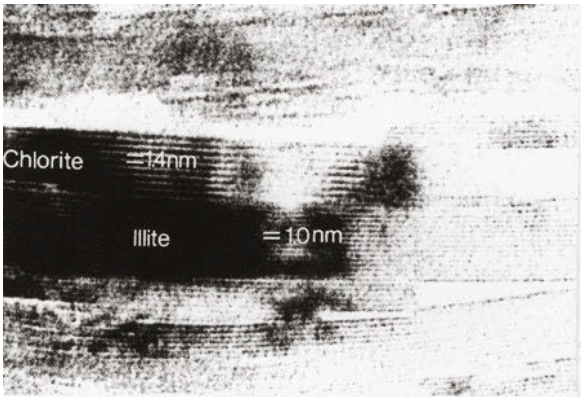

Figure 1. TEM lattice fringe images of the sample from a depth of 548.7 m from well C S 2-14, showing a sharp distinction between well-defined packets of illite (1.0 nm) and chlorite (1.4 nm) layers.

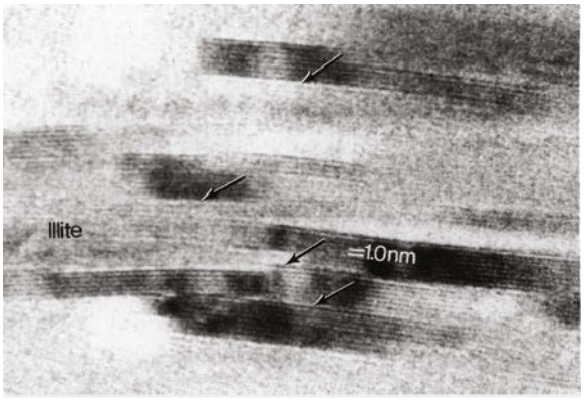

Figure 2. TEM lattice-fringe images of the sample from a depth of 390.6 m from well C S 2-14, showing that illite packets have discrete grain boundaries, packets being related by low-angle boundaries (see arrows).

https://doi.org/10.1346/000986002760833747 Published online by Cambridge University Press

Table 1. Summary of χ^2 tests of CSDs of samples from wells C-S 12 and IDD No. 2.

Figure no.	Well	Observed distribution	Calculated distribution	χ^2 values	Degree of freedom	Significance level (%)
5a	C-S 12	Illite (390.6 m)	Second order kinetics	8.71	10	>20
5a	C-S 12	Illite (446.4 m)	Second order kinetics	3.21	6	>20
5a	C-S 12	Illite (548.7 m)	Second order kinetics	10.58	8	>10
5a	C-S 12	Illite (744 m)	Second order kinetics	3.25	7	>20
5b	IDD No. 2	Illite (485.5 m)	Second order kinetics	2.84	10	>20
5b	IDD No. 2	Illite (1242.9 m)	Second order kinetics	8.56	9	>10
5c	IDD No. 2	Chlorite (485.5 m)	Second order kinetics	59.23	7	>1
6a	C-S 12	Illite (390.6 m)	Log normal (α = 0.003, β^2 = 0.176)	10.52	9	>20
6b	C-S 12	Illite (446.4 m)	Log normal (α = −0.080, β^2 = 0.161)	1.56	6	>20
6c	C-S 12	Illite (548.7 m)	Log normal (α = −0.027, β^2 = 0.118)	6.32	9	>20
6d	C-S 12	Illite (744 m)	Log normal (α = 0.003, β^2 = 0.115)	1.65	8	>20
6e	C-S 12	Biotite (1572.6 m)	Log normal (α = −0.394, β^2 = 0.505)	25.32	17	>5
6f	IDD No. 2	Illite (485.5 m)	Log normal (α = −0.026, β^2 = 0.135)	2.69	10	>20
6g	IDD No. 2	Illite (1242.9 m)	Log normal (α = −0.062, β^2 = 0.127)	2.31	10	>20
6h	IDD No. 2	Chlorite (485.5 m)	Log normal (α = −0.194, β^2 = 0.93)	1.69	7	>20

crystallites to form a small number of apparent single crystals (Baronnet, 1982).

Normalized grain-size distributions of illite at depths of 390.6, 446.4, 548.7 and 744 m from the C S 2-14 well and illite, 485.5 and 1242.9 m, and chlorite, 485.5 m, from the IID No. 2 well, respectively, are plotted in reduced coordinates in Figure 5a,b. The reduced coordinates are $f(r)/f(r)_{max.}$ and r/r_{mean}, where $f(r)_{max.}$ and r_{mean} are maximum frequency of the distribution and mean grain-size, respectively. The solid lines in Figure 5a,b correspond to normalized grain-size distributions as calculated for crystal growth according to second-order kinetics (Baronnet, 1982). The grain-size distributions of illite from both wells are consistent with calculated theoretical profiles for second-order kinetics as indicated by χ^2 tests (Davis, 1973; Krumbein and Graybill, 1965) for which the significance levels (>10% to >20%) are high (Table 1). The calculated profiles are therefore accurate representations of the observed data.

The CSDs of illite at depths of 390.6, 446.4, 548.7 and 744 m and of biotite, 1572.6 m, from the C-S 12 well and of illite at 485.5 and 1242.9 m, and of chlorite at 485.5 m from well IID No. 2 were plotted with calculated log-normal profiles for each depth in Figure 6a–h, respectively. A log-normal distribution can be expressed (Eberl *et al.*, 1998) as:

$$f(\omega) = [1/(\omega\beta(2\pi)^{0.5})] \times \exp\{-(0.5/\beta^2)[\ln(\omega) - \alpha]^2\}$$

where $f(\omega\}$ is the frequency of the observation ω, β^2 is $\Sigma[\ln(\omega) - \alpha]^2 f(\omega)$, the variances of the logarithms of the observations, and α is $\Sigma(\ln\omega)f(\omega)$, the mean of logarithms of the observations. Calculated values of α and β (Table 1) were used to create log normal distributions, using the software statistics program S-PLUS. The solid lines in Figure 6 are calculated profiles, whereas measured grain-sizes are plotted as points. The values listed in Table 1 have high significance levels (>20%), with the exception of those for biotite, demonstrating that the CSDs approximate those of the calculated log normal distributions.

DISCUSSION

Growth conditions of illite, biotite, and chlorite in the SSGF

The sediments in the Salton Sea area are presently undergoing modification through interaction with convecting hydrothermal solutions activated by an unusually high geothermal gradient (Helgeson, 1968; Muffler and White, 1969). It has been active for only ~16,000 years (Kistler and Obradovich, in Muffler and White, 1969). The sequence of clay minerals from well IID No. 2, with increasing depth, is: (1) Surface to ~255.8 mbs: detrital materials, including muscovite, biotite and kaolinite, are undergoing modification to I-S and illite (Giorgetti *et al.*, 2001). Detrital clays are being replaced directly by I-S and illite, but are also undergoing dissolution with crystallization of I-S or illite in pore-space. (2) 255.8–1360 mbs: only illite occurs, having formed through dissolution of detrital minerals, I-S and smectite. The zone of illite overlaps with that of chlorite at greater depth. (3) 439–1515 mbs:

https://doi.org/10.1346/000986002760833747 Published online by Cambridge University Press

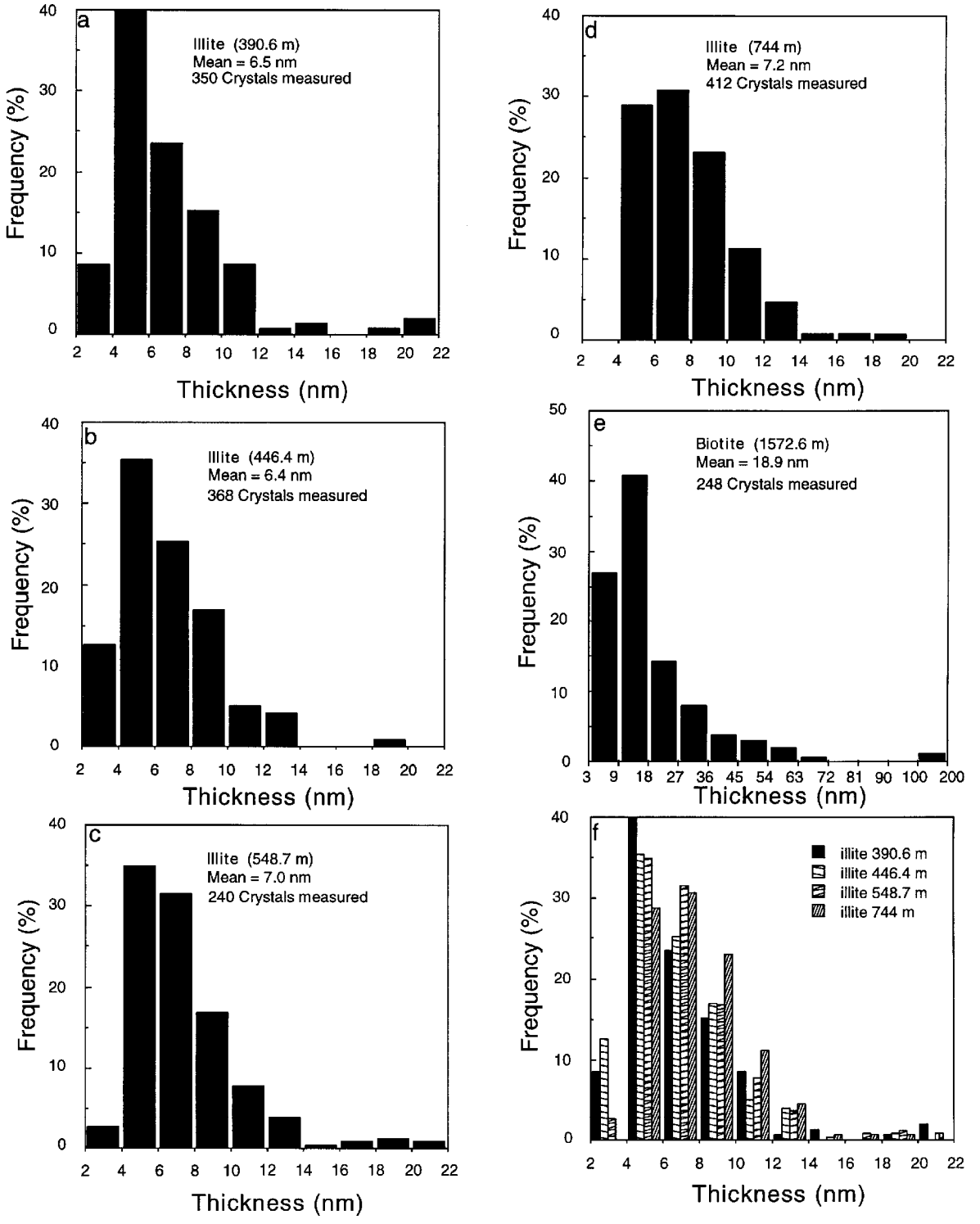

Figure 3. Grain-size histograms of illite from depths of (a) 390.6, (b) 446.4, (c) 548.7 and (d) 744 m, and (e) biotite from a depth of 1572.6 m from well C S 2-14. (f) Grain-size histogram of illite from depths of 390.6, 446.4, 548.7 and 744 m showing that grain-size histograms flatten, broaden and shift to greater sizes with increasing depth.

chlorite occurs, overlapping with zones of illite and biotite at shallowest and greatest depths, respectively. (4) 1258.9–1559.9 mbs: biotite zone.

We are concerned here only with phyllosilicates from the zones of illite, chlorite and biotite, as clay minerals at shallower depths include detrital phases and those

https://doi.org/10.1346/000986002760833747 Published online by Cambridge University Press

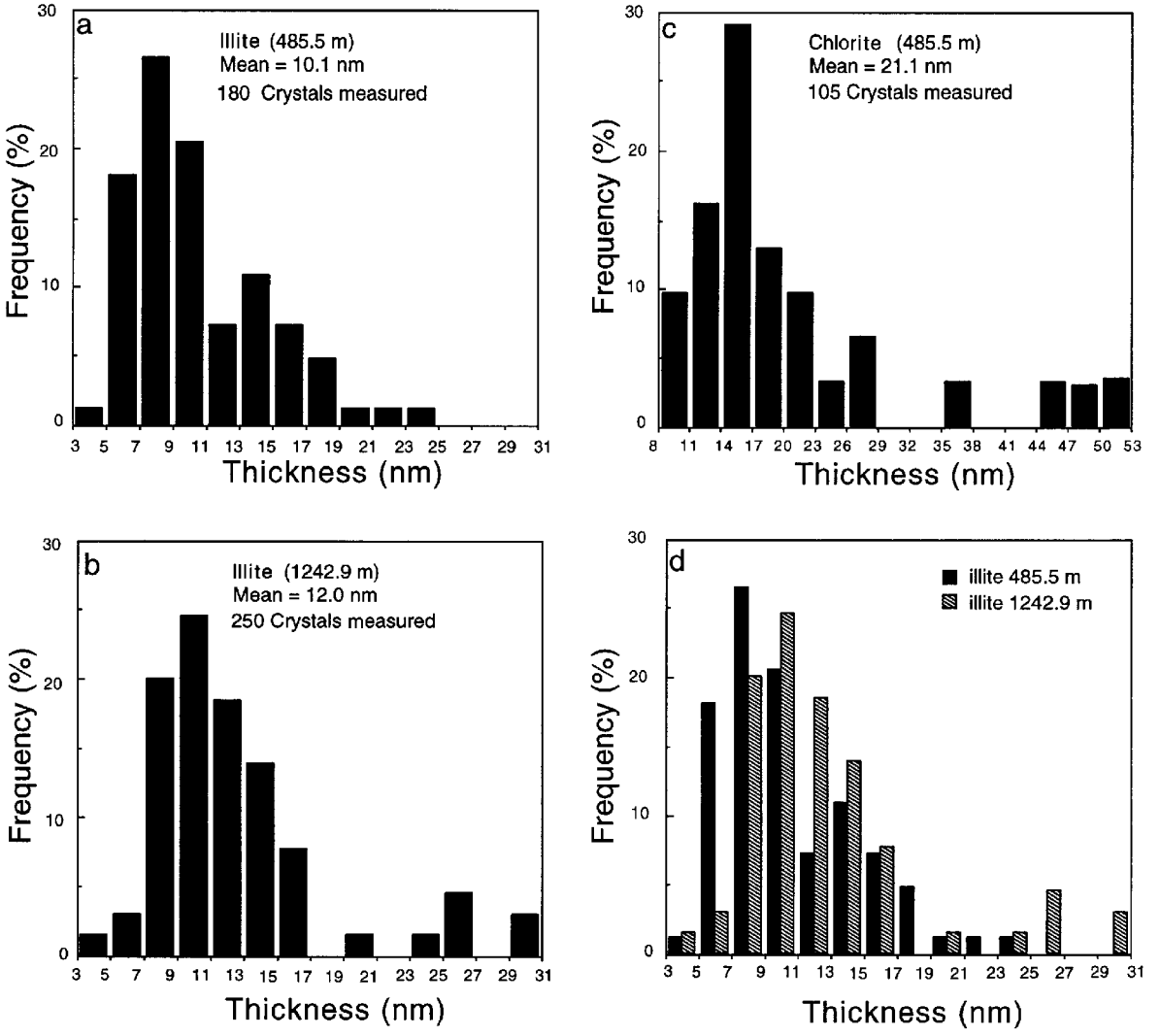

Figure 4. Grain-size histograms of illite from depths of (a) 485.6 and (b) 1242.9 m, and (c) chlorite, 485.5 m, from well IID No. 2. (d) Grain-size histogram of illite from depths of 485.5 and 1242.9 m.

which are transitional to illite; these occur in complex intergrowths with crystal boundaries which cannot be defined easily. Yau *et al.* (1987, 1988) showed, through TEM images of ion-milled samples, that illite, chlorite and biotite occur as packets of (001) layers with sharply-defined boundaries, and thicknesses of ~10 nm. Such packets have the appearance of subparallel laths in cross-section, and only partially fill pore-space. All images of ion-milled SSGF samples observed in the present study show those features and thus permit virtually unambiguous measurement of crystal thickness. This is in sharp contrast with conclusions for shales where individual crystal boundaries are well defined, as described, *e.g.* by Li *et al.* (1998).

Where zones of one clay mineral overlap another, the two minerals occur as separate packets with no evidence of replacement of one by the other. The sequence of phyllosilicates starting with illite, with increasing depth and thus increasing temperature, is typical of a prograde sequence for crystallization in pelitic systems with increasing grade. The collective data thus imply that the minerals formed *in situ*, directly from solution, and without further modification (Giorgetti, 2001); *e.g.* where biotite now occurs, it crystallized directly from fluid whose composition was derived from that of convecting, mobile fluids as modified locally by dissolution of detrital minerals. There is no evidence for prior formation and replacement of the lower-grade clays chlorite and illite.

Relation of Salton Sea clay mineral data to theoretical profiles of Eberl et al. (1998)

Noting that crystal-size distributions of minerals tend to be log normal, Eberl *et al.* (1998) derived theoretical crystal-size distributions for five different growth mechanisms based on the Law of Proportionate Effect.

https://doi.org/10.1346/000986002760833747 Published online by Cambridge University Press

Two of those mechanisms require steady-state conditions as a function of time; *i.e.* normalized CSDs for the evolving system are identical. These are supply-controlled growth in an open system (see below for discussion of unconventional definitions of open and closed systems) and supply-controlled random ripening in a closed system. Both of these mechanisms 'preserve the shape of previous CSD', *i.e.* they involve modification of a distribution produced by some other process involving initial growth. Two such growth processes which produce log-normal CSDs are nucleation and growth with decaying nucleation rate, and surface-controlled growth. Ostwald ripening, for which the total mass of growing and dissolving crystals remains constant, causes an initial log-normal distribution to become more symmetrical, with non-steady-state conditions at least during initial stages.

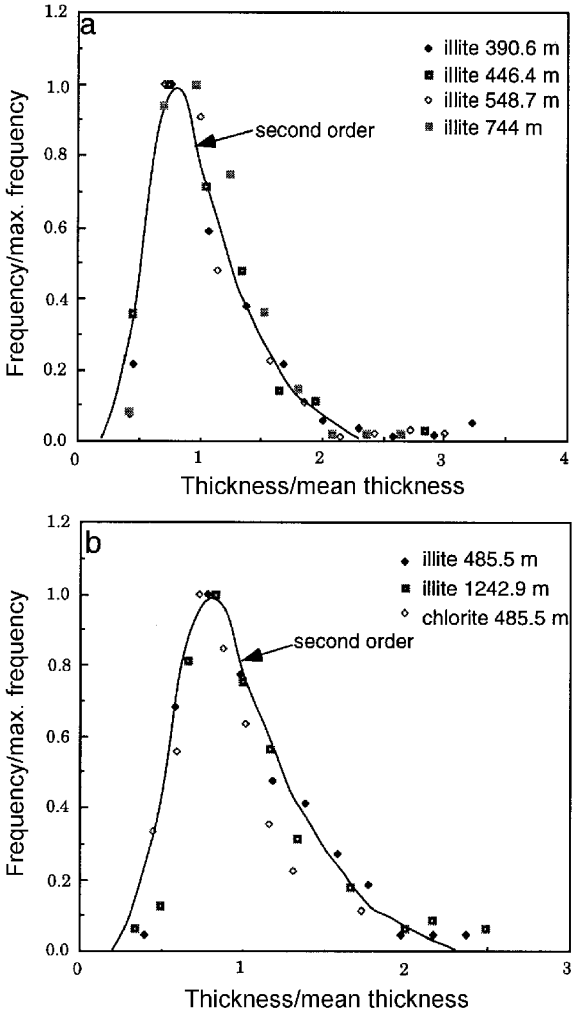

Figure 5. (a) Illite grain-size distributions from well C-S 12, and (b) illite and chlorite grain-size distributions from well IID No. 2, normalized and plotted in reduced coordinates, showing that grain-size distributions fit the theoretical profile (solid line) determined by second-order kinetics.

The CSDs for illite as a function of depth in the SSGF as determined in this study (Figures 5 and 6) are all log normal, and the normalized functions obey steady-state conditions. Of the five functions defined by Eberl *et al.* (1998) they therefore appear to fit the criteria only for initial growth of a log-normal distribution in an open system, followed by growth or modification by either supply-controlled growth or random ripening. Random ripening requires that the total mass of the mineral, for which crystals are growing, remains constant, however, and because fluids are actively convecting and transporting solutes, that mechanism cannot apply. The relations are therefore only consistent with crystal growth in an open system in which a log-normal distribution is produced, followed by supply-controlled growth. Indeed, because the Salton Sea Geothermal System is an open system as defined both by the usual thermodynamic constraints and by Eberl *et al.* (1998), the correspondence between the theoretically-derived CSDs and the observed values would seem to be strong permissive evidence for concluding that the theoretical and natural systems are directly related.

Relevance to geological conditions

The CSDs measured in this study for illite in the SSGF correspond to different depths. Temperature increases with increasing depth, and convecting fluids change composition as they ascend, having interacted with sediments as they were convected. Thus, the conditions for formation of illite are different for each stratigraphic level. Because both temperature and fluid composition affect crystal growth rates, and because all illite at all depths has formed at the same time by direct crystallization from solution, the CSDs at different depths can not be considered to be samples of the same system taken at different times in its evolution. The small increase in mean sizes of illite crystals with increase in depth cannot be ascribed to additional growth or ripening in identical initial systems, therefore, but must be related instead to increase in temperature and/or change in fluid composition. The apparent agreement between measured steady-state conditions and theoretical relations is therefore a necessary condition for supply-controlled growth, but the correlation is fortuitous and not sufficient to define such a mechanism. On the other hand, the individual CSDs are consistent with the model of Eberl *et al.* (1998) for initial growth in an open system. Their definition of an open system (see below) is compatible with the thermodynamic definition in this case where solvents are transported by convecting fluids. The individual distributions thus agree nicely with the distribution as predicted by Eberl *et al.* (1998).

Aspects of CSDs in natural systems in relation to laboratory systems

Many studies of crystal growth have been carried out which are based on crystallization in the laboratory

https://doi.org/10.1346/000986002760833747 Published online by Cambridge University Press

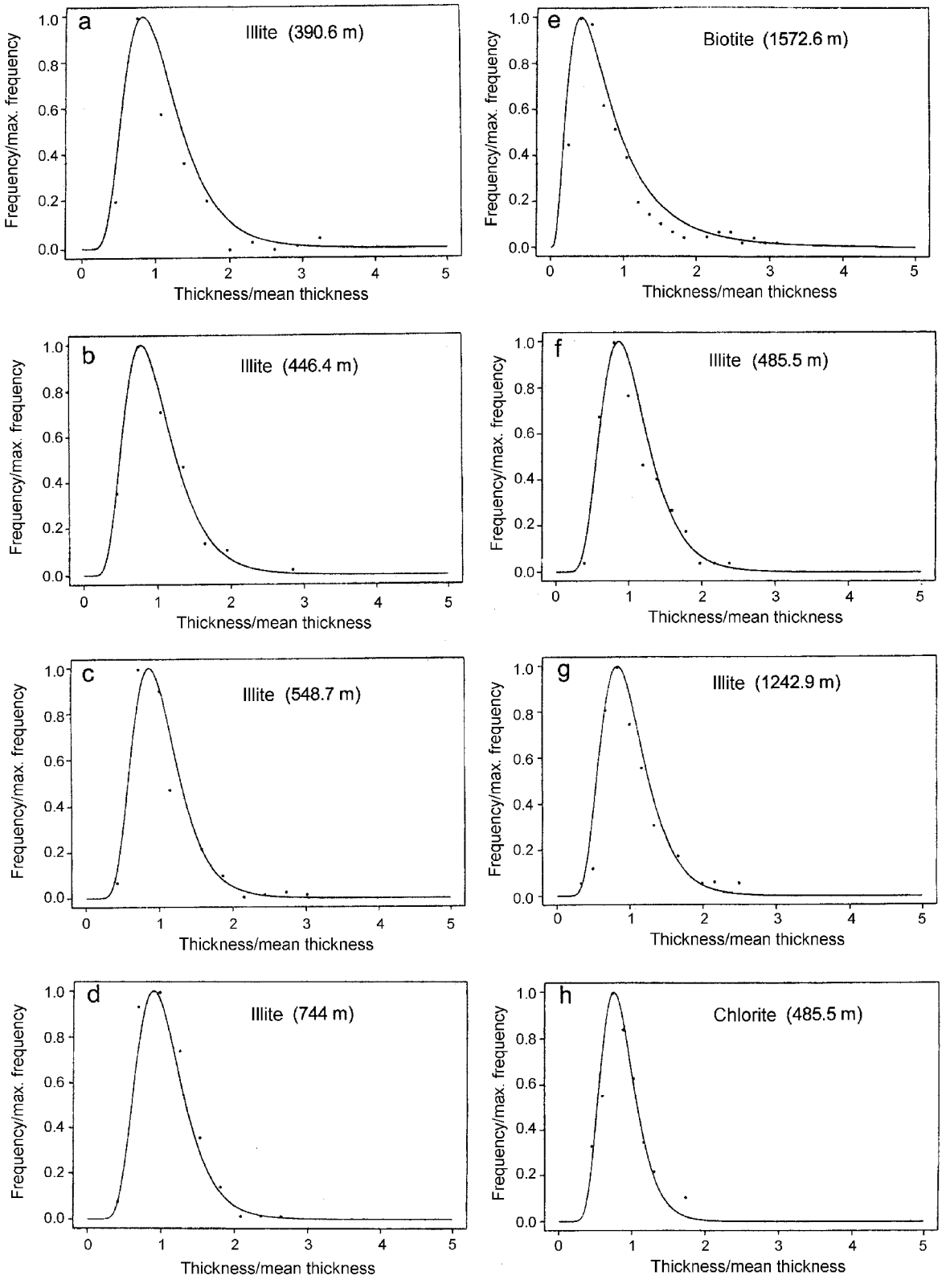

Figure 6. Grain-size distributions for illite from depths of (a) 390.6, (b) 446.4, (c) 548.7, (d) 744 m, and (e) biotite, 1572.6 m from well C-S 12, and illite, (f) 485.5 and (g) 1242.9 m, and (h) chlorite, 485.5 m from well IID No. 2, plotted with calculated log-normal profiles (solid line) for each depth.

(Eberl *et al.*, 1998, and references therein). Such studies permit sampling of a single system at constant temperature under thermodynamically-defined closed- or open-system constraints as the system evolves. It is therefore possible to test for steady-state conditions. In addition, Eberl *et al.* (1998) showed how the log-normal parameters α and β^2 evolve for their five growth mechanisms. It is therefore possible to compare such theoretical trends with the observed trends.

Natural systems do not generally permit one to sample a given rock system as a function of time. It is therefore generally not possible to measure the evolution of CSDs of a given system. As with this study of Salton Sea sediments, samples are generally obtained in sequences over which there is inevitably a change in conditions. Such is the case, for example, in basin sediments where temperature and fluid composition evolve as a function of depth. There is a kind of 'catch 22' in the analysis of geological materials in that one seeks sequences over which there are differences, but those differences are invariably a function of some variable other than simply time. The conditions for testing for trends in the log-normal parameters α and β^2 as a function of time in an evolving geological system must be rare.

It is also commonly assumed that, because clay minerals evolve through predictable sequences as a function of depth in sedimentary basins, for example, that a more evolved clay mineral will have progressively evolved through all of the states represented by less evolved clay minerals, *e.g.* those at shallower depths in sedimentary sequences. Some sequences of clay minerals in hydrothermal systems have recently been inferred to be episodic in nature, *i.e.* clays of all stages of reaction progress have formed by direct precipitation from fluids, without necessarily having been preceded by a clay mineral of lesser reaction progress (Yan *et al.*, 2001; Tillick *et al.*, 2001; and references therein) as is the case for the Salton Sea system. There are significant radioisotope data implying that even in Gulf Coast sediments, which are considered by many to be a 'type' section of continuous transformations as a function of time (Hower *et al.*, 1976), diagenesis may be episodic, *i.e.* the small increase in crystallite size of illite as a function of depth, as inferred by Hower *et al.* (1976) and verified by R.J. Merriman (pers. comm.) on the basis of TEM observations, may have been caused by variable temperature for simultaneous crystallization of at least some illite at different depths. Such a notion is contrary to widely accepted dogma. We do not advocate it as necessarily applicable to any but the hydrothermal systems for which observations directly support the idea. We do suggest, however, that progressive transformations as a function, say of depth, should not automatically be assumed to represent time-dependent functions; as in the case of the Salton Sea system, CSDs measured for different degrees of reaction progress may, therefore, not be comparable as snapshots in the progress of identical systems. For this and other reasons, we therefore urge caution in drawing conclusions about crystal-growth mechanisms based on comparison of theoretical distributions with natural ones. Indeed, we find it difficult to imagine any natural clay-mineral system where evolution of CSDs as a function only of time can be studied.

We therefore infer that the CSDs of this study cannot be compared as representing different stages of a single evolving process. Rather we interpret each of them as representing a stage in direct growth in an open system for which simultaneous growth conditions differed for each sample. The data represent crystallization in a simple, well-constrained, open geological system, however, and should therefore serve as a standard for such relations. Insofar as the CSDs for all SSGF samples, including those for chlorite and biotite, are log normal and represent direct precipitation from solution, they are compatible with two of the growth mechanisms for open systems as defined by Eberl *et al.* (1998), namely nucleation and growth with decaying nucleation rate and surface-controlled growth.

Open vs. closed systems

The Salton Sea system is considered to be an 'open' system (*e.g.* Yau *et al.*, 1988) in the normal geological context. That context is based on strict definitions of system openness or closure in the thermodynamic sense. As such, it is necessary to first define a 'system', which is done by establishing boundaries. An open system is therefore one where chemical components (also as strictly defined) pass across the boundaries, whereas a closed system is one where no material is exchanged with the surroundings.

Eberl *et al.* (1998), however, have chosen to differentiate growth mechanisms on the basis of 'open' and 'closed' systems which are partially inconsistent with conventional meanings. They define an open system, for example, as one where reactants and products are different phases, the amount of the product mineral increasing with time, whereas they define a closed system as one in which some crystals of a given mineral dissolve and some increase in size, thus maintaining the total mass of that phase. But a system in the chemical sense must include all phases within it, and cannot consist of separated phases, *e.g.* the fluid and all other minerals are part of the system which would be defined by considering one or more phases, say growing illite.

The terms 'open system' and 'closed system' are generally well understood by geological scientists in a thermodynamic context, and their meanings are unambiguous. Use of those terms in entirely different ways for the same systems where those terms are used in a normal chemical sense, creates confusion. Indeed, in describing these relations herein we have used those terms with

some difficulty because of their double meanings. We therefore suggest use of the terms 'constant and variable mass of a phase' in place of 'closed and open system', respectively, or some such, to eliminate potential confusion, with retention of the latter terms in their normal thermodynamic and geological sense.

ACKNOWLEDGMENTS

We acknowledge financial support from NSF grants EAR-91-04565 and EAR-98-14391 to Donald R. Peacor. We thank Dr J.W. Morse, Dr Jan Środoń, Dr D. McCarty, D.D. Eberl, and A. Baronnet for constructive reviews. Part of the work was performed while the first author held a CORE/NRL Postdoctoral Fellowship.

REFERENCES

Árkai, P., Merriman, R.J., Roberts, B., Peacor, D.R. and Toth, M.N. (1996) Crystallinity, crystallite size and lattice strain of illite-muscovite and chlorite: comparison of XRD and HRTEM data for diagenetic to epizonal pelites. *European Journal of Mineralogy*, **8**, 1119–1137.

Baronnet, A. (1982) Ostwald ripening in solution. The case of calcite and mica. *Estudios Geologie*, **38**, 185–198.

Davis, J.C. (1973) *Statistics and Data Analysis in Geology*. John Wiley & Sons, Inc., New York, 550 pp.

Donaghe, L.L. and Peacor, D.R. (1987) Textural and mineralogic transitions in SSSDP argillaceous sediments. Abstract, *EOS, Transactions of the American Geophysical Union,* **68**, 454.

Eberl, D.D. and Środoń, J. (1988) Ostwald ripening and interparticle-diffraction effects for illite crystals. *American Mineralogist,* **73**, 1335–1345.

Eberl, D.D., Środoń, J., Kralik, M., Taylor, B.E. and Peterman, Z.E. (1990) Ostwald ripening of clays and metamorphic minerals. *Science,* **248**, 474–477.

Eberl, D.D., Drits, V.A. and Środoń, J. (1998) Deducing growth mechanism for minerals from the shapes of crystal size distribution. *American Journal of Science,* **298**, 499–533.

Giorgetti, G., Mata, M.P. and Peacor, D.R. (2001) TEM study of the mechanism of transformation of detrital kaolinite and muscovite to illite/smectite in sediments of the Salton Sea Geothermal Field. *European Journal of Mineralogy*, **12,** 923–934.

Helgeson, H.C. (1968) Geologic and thermodynamic characteristics of the Salton Sea Geothermal System. *American Journal of Science,* **266**, 129–166.

Hower, J., Eslinger, E.V., Hower, M. and Perry, E.A. (1976) Mechanism of burial metamorphism of argillaceous sediment: 1. Mineralogical and chemical evidence. *Geological Society of America Bulletin*, **87**, 725–737.

Inoue, A., Velde, B., Meunier, A. and Touchard, G. (1988) Mechanism of illite formation during smectite-to-illite conversion in a hydrothermal system. *American Mineralogist*, **73**, 1325–1334.

Jahren, J.S. (1991) Evidence of Ostwald ripening related recrystallization of diagenetic chlorites from reservoir rocks offshore Norway. *Clay Minerals,* **26**, 169–178.

Krumbein, W.C. and Graybill, F.A. (1965) *An Introduction to Statistical Models in Geology*. McGraw-Hill Book Company, New York, 475 pp.

Lanson, B. and Champion, D. (1991) The I/S-to illite reaction in the late stage diagenesis. *American Journal of Science*, **291**, 473–506.

Li, G., Peacor, D.R., Buseck, P.R. and Arkai, P. (1998) Modification of illite-muscovite crystallite-size distribution by sample preparation for powder XRD analysis. *Canadian Mineralogist,* **36**, 1435–1451.

Muffler, L.P.J. and White, D.E. (1969) Active metamorphism of Upper Cenozoic sediments in the Salton Sea geothermal field and Salton trough, southeastern California. *Geological Society of America Bulletin*, **80**, 157–182.

Nielsen, A.E. (1964) *Kinetics of Precipitation*. Pergamon Press, New York, 151 pp.

Ostwald, W. (1900) Uber die vermeintliche Isomerie des roten und gelben Quecksilberroxsyds und die Oberflachenspannung festter Korper. *Zeitschrift fur Physikalische Chemie, Stoichiometrie und Verwandtschaftslehre*, **34**, 495–503.

Peacor, D.R. (1998) Implication of TEM data for the concept of fundamental particles. *The Canadian Mineralogist,* **36**, 1397–1408.

Tillick, D.A., Peacor, D.R. and Mauk, J.L. (2001) Genesis of dioctahedral phyllosilicates during hydrothermal alteration of volcanic rocks: I. The Golden Cross epithermal ore deposit, New Zealand. *Clays and Clay Minerals*, **49**, 136–140.

Yan, Y., Tillick, D.A., Peacor, D.R. and Simmons, S.F. (2001) Genesis of dioctahedral phyllosilicates during hydrothermal alteration of volcanic rocks: II. The Broadlands-Ohaaki hydrothermal system, New Zealand. *Clays and Clay Minerals*, **49**, 141–155.

Yau, Y.C., Peacor, D.R. and McDowell, S.D. (1987) Smectite-illite reactions in Salton Sea shales. *Journal of Sedimentary Petrology*, **57**, 335–342.

Yau, Y.C., Peacor, D.R., Beane, R.E. and Essene, E.J. (1988) Microstructures, formation mechanisms, and depth-zoning of phyllosilicates in geothermally altered shales, Salton Sea, California. *Clays and Clay Minerals*, **36**, 1–10.

(*Received 27 December 1999; revised 2 November 2001; Ms. 417; A.E. Douglas K. McCarty*)